# Precise Vehicle Topology and Road Surface Modeling Derived from Airborne LiDAR Data

Charles K. Toth[1], Dorota A.Grejner-Brzezinska[2] and Shahram Moafipoor[1]

[1] *Center for Mapping, The Ohio State University*
*1216 Kinnear Road, Columbus, OH 43212*

*Tel: 614-292-7681; Fax: 614-292-8062*
*e-mail: toth@cfm.ohio-state.edu*

[2]*Department of Civil and Environmental Engineering and Geodetic Science*
*470 Hitchcock Hall, 2070 Neil Avenue*

## BIOGRAPHY

Dr. Charles Toth is a Senior Research Scientist at the Ohio State University Center for Mapping. He received an MS in Electrical Engineering and a Ph.D. in Electrical Engineering and Geoinformation Sciences from the Technical University of Budapest, Hungary. His research expertise covers broad areas of 2D/3D signal processing, spatial information systems, high-resolution imaging, surface extraction, modeling, integrating and calibrating of multi-sensor systems, multi-sensor geospatial data acquisition systems, and mobile mapping technology. He is Co-Chairing ISPRS WG II/2 on LiDAR and InSAR Systems and serves as the Assistant Director for the Photogrammetric Application Division of ASPRS.

Dr. Dorota Brzezinska is an Associate Professor in Geodetic and Geoinformation Science, The Ohio State University (OSU). Prior to that, she was a Research Specialist at the OSU Center for Mapping. She received an MS in Surveying and Land Management from the Agricultural and Technical University of Olsztyn, Poland, and an MS and a Ph.D. in Geodesy from OSU. Her research interests cover precise kinematic positioning with GPS, precision orbit determination for GPS/LEO, GPS/INS integration, mobile mapping technology, and robust estimation techniques. Between 1990-1995 she was a Fulbright Fellow at OSU. She is the 2003-2005 Land Representative for the ION Council, chair of IAG Sub-Commission 4.1, *Multi-sensor Systems*, a co-chair of the IAG Study Group 4.1, *Pseudolite Applications in Positioning and Navigation*, and a chair of the Task Force 5.3.1, *Mobile Mapping Systems* of FIG WG 5.3.

Mr. Shahram Moafipoor is a PhD student in the Department of Geodetics Science, The Tehran University, and currently he is a visiting scholar in the Department of Civil and Environmental Engineering and Geodetic Science, The Ohio State University. Prior to that, he was a researcher at National Cartography Center NCC, Iran. He obtained an MS degree in photogrammetry from Tehran University in Tehran, Iran in 1998 and B.Sc in surveying from Tehran University in Tehran, Iran in 1993. His research interests include navigation systems, aerial photography, and digital photogrammetry.

## ABSTRACT

This paper represents the continuation of research presented earlier (Grejner-Brzezinska and Toth, 2002 and 2003a-b; Toth et al, 2003 a-b) referred to a theoretical and practical study on the feasibility of using LiDAR (Light Detection and Ranging) data and airborne imagery collected simultaneously over the transportation corridors for obtaining traffic flow estimates, such as (1) vehicle count estimates based on extracting vehicles from dense LiDAR point cloud and/or imagery, (2) classification of extracted vehicles into main categories, (3) velocity estimates based on modeling the vehicle categories and using sensor navigation data, and (4) intersection movement patterns.

In this paper, we present the updated algorithms and methodology of extracting the vehicle information together with the road surface modeling with precisely georeferenced (GPS/INS) LiDAR data, augmented by LiDAR intensity information. We demonstrate that intelligent algorithms that we developed are capable of fast and robust identification of the shapes (especially the vertical profiles of the vehicles), proving LiDAR's ability to preserve the vehicle geometry better, as compared to conventional image projection (again, primarily the vertical profile), where it can be significantly distorted. We prove that if LIDAR data of sufficient spatial density are available, vehicle extraction and their coarse classification can be efficiently performed in parallel to the efficient and automated road surface extraction and modeling.

## 1. INTRODUCTION

Federal and local government transportation management services monitor and control the traffic over the urban road network and the nation's highway system. These agencies collect data for both long-term planning and real-time traffic control. Real time information is usually gathered from many diverse sources, such as electronic sensors in the pavement (loop detectors), road tubes, ramp meter sensors, and video and digital cameras, which are sent to the traffic management center at various times. Most of this information is only recorded; a small part of it is analyzed in real-time and used for immediate traffic control and decision making. Commonly, the density and flow of traffic are the two main parameters for describing the traffic stream. In simple terms, the density is the number of vehicles occupying a road lane per unit length at a given time, while traffic flow represents the amount of vehicles traveling over a road segment in a given time period.

With the increasing number of vehicles entering the current transportation network annually, the importance of effective traffic management is becoming more crucial, because the construction of new roads is not keeping up with the volume of growing traffic. The key to better traffic management, however, is the access to better data and, of course, the capability for immediate processing of the data to provide a real-time response. Therefore, interest in new sensors that can provide large volumes of data in real-time is steadily growing. Airborne and spaceborne remote sensing technology can provide data in large spatial extent with varying temporal resolution. One of the distinctive characteristics of using remote sensing is that it can be deployed more or less anytime and anywhere – a definite advantage over the spatially local sensors. The installation and use of ground-based sensors disrupts traffic and endangers the crews.

LiDAR has become the primary surface extraction technology in mapping in the last five years. Its success is mainly due to the high-level of automation offered – the data can be literally used as acquired; the need for interactive processing is usually very limited. Mapping of the transportation infrastructure is primarily concerned with the static part of the object space. Vehicles, in particular the moving ones, pose a difficulty for processing: these objects should be removed during the processing. Instead of throwing away the removed objects, it could be advantageous to use these data to derive valuable information for traffic monitoring and management. An earlier research investigated the feasibility of extracting vehicles and classifying them into main groups, see (Grejner-Brzezinska *et. al*, 2003 and 2004; Toth et al, 2003b; Toth and Grejner-Brzezinska, 2004). Based on the success of the initial study, the decision was made to further investigate the approach and to develop a prototype of the concept. This paper reports additional research components not addressed in the initial phase.

## 2. SYSTEM DESIGN

The processing architecture of the system automatically extracting traffic flow from LiDAR data is shown in Fig. 1. The main processing steps are: (1) road surface extraction, (2) vehicle extraction, (3) primary parameterization of the vehicle shape – vehicle modeling, (4) feature space selection – parameter optimization, (5) vehicle classification, (6) vehicle velocity estimates, and (7) traffic flow data computation. The initial feasibility research on extracting flow data from LiDAR was focused on tasks (3-5). In this paper, the other tasks, which are the subject of ongoing research, are discussed. Section 3 is concerned with the road surface extraction. The primary objective is to determine the road boundaries while the complete surface modeling is omitted. Vehicle extraction is based on the availability of the road footprint and is discussed in Section 4. The aspects of vehicle velocity estimates are introduced in Section 5. Using an actual data set from a conventional LiDAR survey, traffic flow results are derived and discussed in Section 6. Finally, the conclusion and remarks are presented.

## 3. ROAD OUTLINE EXTRACTION

At a small scale roads are considered as linear features, while in large scale they are typically characterized by centerline and width parameters in 2D or by additional slope parameter in 3D. Furthermore, road details such as edge lines, median, fences, concrete dividers, shoulder lines, traffic signs, etc, are available at engineering scale mapping. The actual pavement surface is rarely modeled as the description using linear features is generally satisfactory.

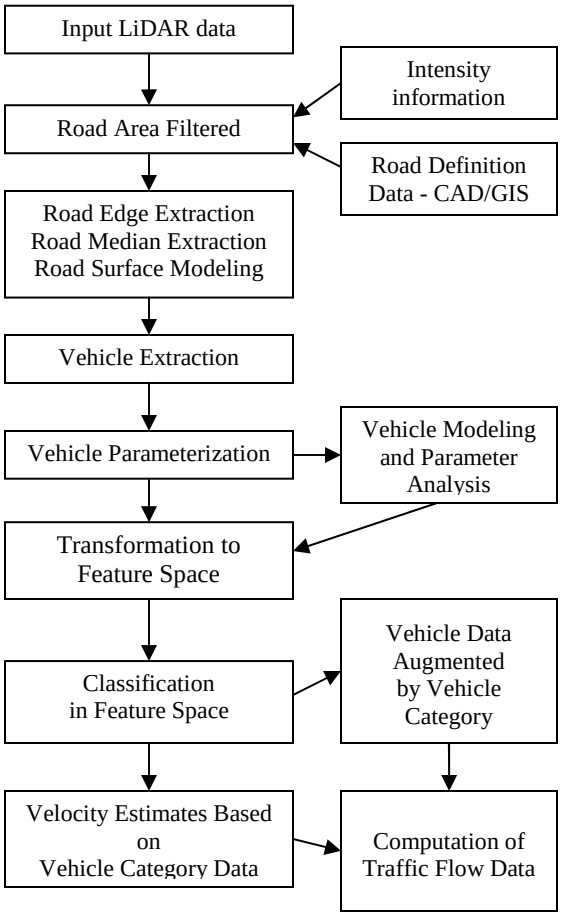


**Figure 1.** Data processing architecture

Methods for road extraction from remote sensed data are available and typically focused on linear feature extraction from satellite or airborne imagery. Extracting roads from LiDAR is a rather new approach (Hu and Tao, 2004). In both cases, however, the identification and coarse delineation of the road is the objective and no consideration is given to pavement level modeling. Also, these techniques are based on a general approach of not assuming the availability of any road data, such as a GIS or CAD database. In reality, this type of data is always available for the developed part of the world. Therefore, the road outline extraction process should be facilitated by using such data, which, in turn, changes the objective from finding roads in LiDAR data to realigning the road description based on the new measurement.

In our concept, the road outline and surface extraction, shown in Fig 2, assume the availability of coarse road data; at a minimum centerline information is needed (e.g.,. from a GIS database). Then the LiDAR point cloud, 3D points, and, depending on availability, LiDAR intensity form the input data. The use of intensity data is still in its infancy, but new systems already offer this capability and therefore are considered here. Approximated road areas/corridors can be separately analyzed based on both data sets and then results can be combined.

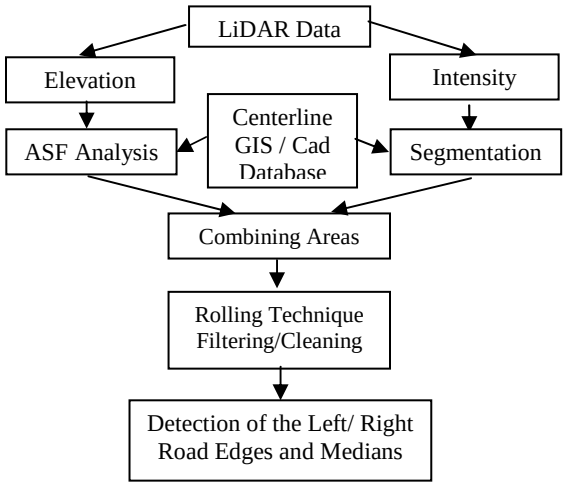


**Figure 2**. The road boundary extraction process

The strength of LiDAR data comes from the true 3D description of the object space, which offers a better object characterization and results in a better feature extraction performance. For our situation, corridor mapping, there are two apparent approaches: (1) segmentation of LiDAR data to find flat surfaces, and (2) analyzing LiDAR scanlines to find straight line segments. In the first case, points are grouped and small surface patches are fit to them, which are described by a plane representation, see Eq. 1.

$$AX + BY + CZ + D = 0 \quad (1)$$

Analyzing the normal vector, $\vec{n} = (A, B, C)$ the patches can be marked as possible road segments. Depending on the quality of the GIS/CAD road data, the road slope information should be used during the processing. If only horizontal data are available, the normal vector should be split into two components, along the road and across the road. The across the road component, which should describe a nearly horizontal surface, should be given higher weight in the segmentation. The along the road components can fluctuate more, but the rate of change should be consistent. This approach works well but is rather computation expensive.

Since roads are usually surveyed with perpendicular scanlines in a typical corridor mapping LiDAR mission, analyzing the road cross profiles as they are measured by consecutive scans provides a good alternative for road detection (changes in geometry are larger in that direction). In fact, this is the reason that roads are conventionally modeled by cross profiles. The basic concept is finding flat segments of the scanlines that correspond to road surfaces. There are several techniques for measuring the roughness and roughness length of a profile such as auto-covariance, cross-correlation, variogram, texture analysis and the fractal method (Thomas, 1999). The correlation between points on a profile, as a random variable, is chosen in this paper and the auto-covariance function or its modified equation called structure function is used in our investigation. For a profile of length *L*, the structure function is defined as:

$$S(\tau) = \frac{1}{L-\tau} \int_0^{L-\tau} \{z(x) - z(x+\tau)\}^2 \, dx \qquad (2)$$

where, *z(x)* and $z(x+\tau)$ are pairs of height values separated by a distance $\tau$. This function is often normalized as the auto-structure function, called ASF:

$$ASF(\tau) = \frac{S(\tau)}{\max(S)} \qquad (3)$$

Figure 3 shows a few consecutive profile lines and the computed ASF functions. Although the ASF computation inherently implements some smoothing, a filtering of either the raw data or the derived ASF function is recommended, as the LiDAR data usually come with noise; typically 5 cm RMS.

The ASF function can be extended for surface patches (2D), but again at the price of increased computation requirements. In our experiences, both methods showed good results, as long as the roads to be identified had distinct geometry with respect to their surroundings. Thus, flat paved areas, such as parking lots and pedestrian walkways, cannot be reliably distinguished from roads. In addition, vehicles obviously cause problems, and therefore, the along the road pattern of the ASF function should be monitored to detect affected lines and they should be removed from the processing. If the scanlines are not perpendicular to the road centerline direction, cross profiles can be computed by interpolation before processing.

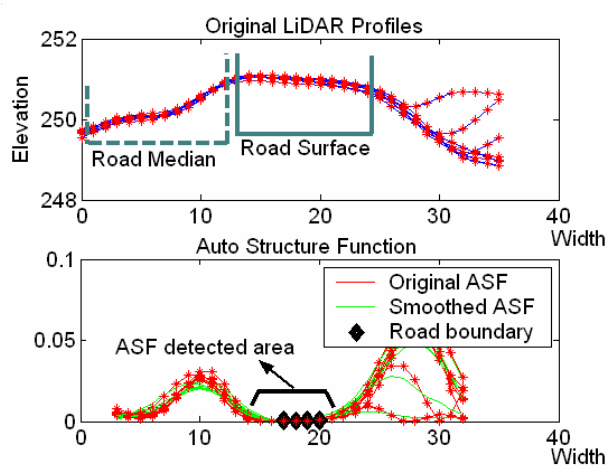


**Figure 3.** The road cross-profiles (top) and the computed ASF showing surface roughness (bottom).

As LiDAR intensity data are becoming widely available, they can be used as an additional source of information for the road extraction. Although the intensity information is relative by nature, it can provide for accurate local segmentation of LiDAR data. For example, the road surface and vegetation along the road exhibit very different signal response; thus segmentation can be based on the relative intensity value. Figure 4 depicts sample data segmented by a 40% intensity threshold value, showing a very good performance. Note the road centerline points, marked in blue, from the GIS/CAD data. The points erroneously segmented can be removed by basic morphology processing.

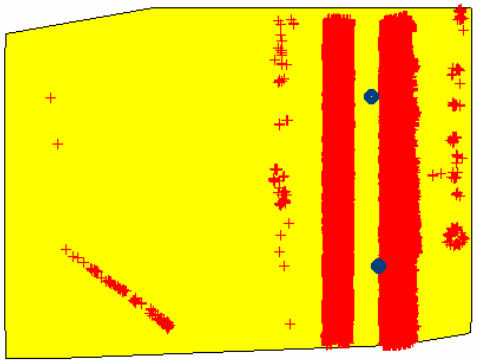

**Figure 4.** Road estimation based on intensity segmentation

Once the road surface areas have been approximated from elevation and intensity (if available) data, a final consistency check using object space constraints should take place to determine and delineate the road. At this point the

road direction and width are approximately known, and the objective is to determine the edge lines of the road. As the changes in road geometry are limited in the road direction, a similarity analysis is performed over smaller road segments, which is defined as a distance comparable to the road width. This technique is called rolling procedure and is based on auto-correlation – basically a virtual bar, parallel to the road direction is rolled from the center of the road towards the edges, see Fig. 5. The rolling of the bar is supposed to stop at the road edges, delineating the road boundaries.

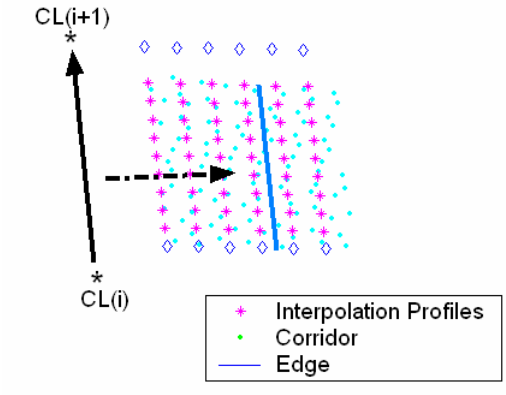


**Figure 5.** Rolling technique

The rolling process works with an overlap to achieve smooth road boundary delineation. Fig. 6 shows final road edges overlaid over the point cloud. The locations were independently formed on the left and right sides of the road.

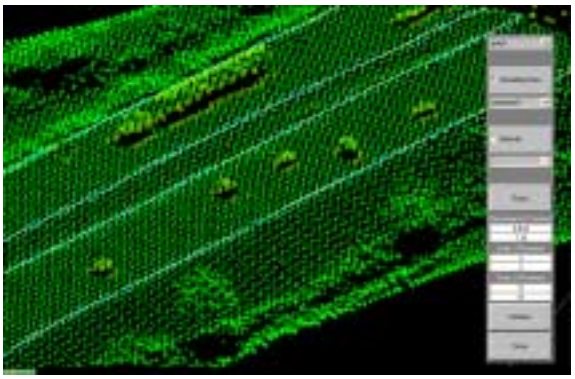

**Figure 6.** Road edges delineation

## 4. VEHICLE REMOVAL AND ROAD MODELING

Once the road boundaries are available, a simple thresholding can extract the vehicles; segments of the road between edge lines are approximated by a plane. To follow the changes in road surface orientation, the thresholding scheme should be adaptive, which guarantees that candidate points representing a vehicle will have true perpendicular height values with respect to the actual road surface – this way the very same vehicle description is obtained no matter whether the road is horizontal or of steep grade. Fig. 7 shows point clusters extracted as vehicle candidates. Note that besides the vehicles, there are other extracted objects that are definitely not vehicles, such as vegetation or guide rails on the side, and thus should be removed during subsequent processing.

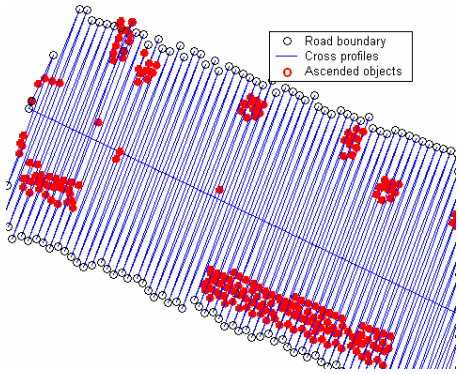


**Figure 7.** Thresholding the ascended points along the scanlines to detect vehicle objects

The vehicle candidate point clouds are modeled to support both vehicle classification and blunder detection – the removal of any raised objects that are not vehicles. As the current LiDAR point density, ranging typically between 1-5 points/m$^2$, and the relatively sizeable footprint size of the laser beam, usually in the range of 10-30 cm, cannot allow for very precise geometrical description of the vehicles, thus only coarse parameterization is possible of the vehicles. For instance, determining the 3D envelope of the vehicle points and then describing it by length, width and height(s) parameters. In addition, derived parameters, such as vehicle footprint size or volume, can be used. Figure 8 depicts vehicle points, showing both LiDAR scanlines and actual points.

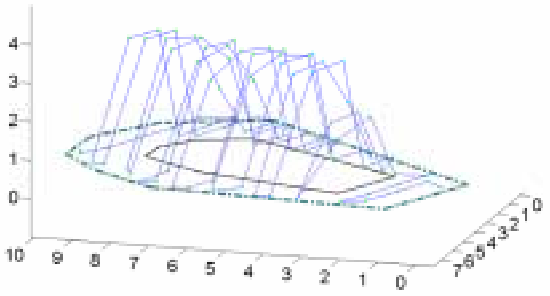

**Figure 8.** Vehicle points extracted with original scanlines overlaid.

Using the basic vehicle parameters, a blunder detection process is executed to remove all non-vehicle objects. Vehicle length varies as a function of the relative speed between a vehicle and the LiDAR sensor platform, but the width is invariant and thus provides the first criterion for blunder detection. Fig. 9 shows a concrete structure separating the two sides of the road that can be easily discarded, as its width falls below the minimum vehicle width and it has an unlikely long length. Additional filters are based on footprint size and volume.

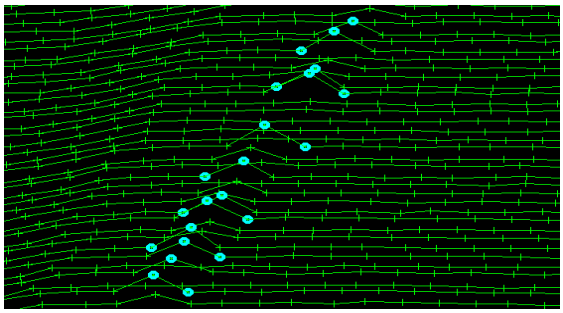

**Figure 9.** Concrete wall, a blunder object.

Once all the likely non-vehicle objects are removed, the next objective is the classification of the vehicles. The original vehicle parameter space, however, does not offer an efficient classification domain, as its dimensionality is high and the parameter correlation is unknown. Therefore, a Principal Component Analysis (PCA) is preferred to arrive at a reduced feature space where the classification takes place. A variety of parameter combinations have been tested such as using width, length, area and volume, or width, length and height profile; or only height profile, e.g., modeled by four values along the vehicle motion direction; and similar parameters augmented by average intensity values. Detailed results can be found in (Toth *et al.*, 2003b). Fig. 10 shows the 2D classification space, based on four parameter modeling, determined by a 72 vehicle training data set. The vehicle classes are passenger cars, trucks and all other vehicles.

The classification performance was tested on different data sets, and in general showed a good performance. From the three classifiers investigated, i.e., the rule-based, the Voronoi tessellation, and the neural network, the first one provided the best performance, consistently achieving about 98% success rate, see (Toth *et al.*, 2003a). It is important to note that the direction of the vehicle motion can also be recovered in some cases. Finally, the use of intensity data did not result in a better classification performance.

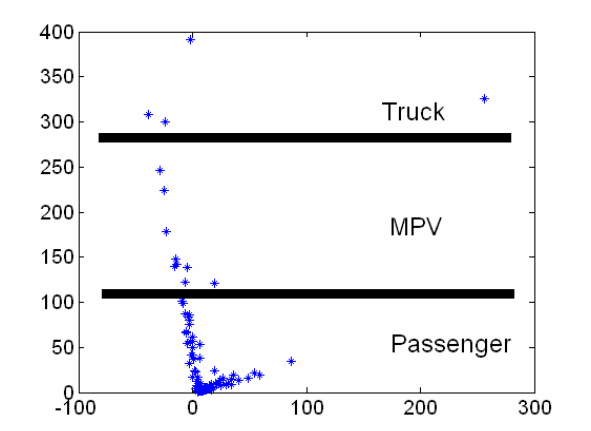


**Figure 10.** The PCA classification of the vehicles in the 2D space

## 5. VELOCITY ESTIMATES

The vehicle velocity is the second parameter needed to compute the traffic flow. The individual speed of each vehicle is usually not of interest, as only the average velocity of a group of vehicles is needed to obtain flow data. In the context of LiDAR, the dependency of the vehicle length with respect to the relative velocity between the object and the sensor forms the basis for speed estimation. Due to the continuous scanning, the vehicles appear shorter or longer in the relative motion direction. Equation (4) describes the relation between the actual size, *s*, and measured size, *m,* of the vehicles moving in both directions:

$$V_{veh} = \frac{m-s}{m} V_{LiDAR} \sin(\theta)\Big|_{along} \qquad (4)$$
$$V_{veh} = \frac{s-m}{m} V_{LiDAR} \sin(\theta)\Big|_{against}$$

where $V_{LiDAR}$ is the velocity of LiDAR platform, $V_{veh}$ is the vehicle velocity and $\theta$ is the intersection angle of LiDAR scan line and vehicle direction, usually small enough, so it can be ignored.

The determination of the vehicle direction is rather obvious, as vehicles always travel on the same side of the road. But, if needed, a simple statistics can show that on one side of the road the sensed length of the vehicles is longer than on the other one. Similarly, the LiDAR platform speed is known at high accuracy. The size parameters, however,

have significant errors. First, the LiDAR footprint has a non-negligible size. Then the LiDAR scanlines are separated by an even larger distance and thus setting a lower limit for the accuracy of the length estimation. Second, the actual vehicle size is unknown; only broad vehicle categories are determined in the classification phase. Therefore, only a size distribution is available for the computation. According to a study by Ramprakash, 2003, the percentage of the passenger car vehicle market share in the USA with corresponding length and height parameters is shown in Table 1.

| Passenger car type | Share [%] | Average length [m] | Average height [m] |
|---|---|---|---|
| Small | 27% | 4.36 | 1.37 |
| Mid size | 49% | 4.73 | 1.36 |
| Large | 9% | 5.23 | 1.38 |
| Luxury | 15% | 4.77 | 1.35 |
| Average | | **4.68 ± 0.35** | **1.36 ± 0.01** |

**Table 1**. The basic statistics of the US passenger car vehicle market

Based on the average vehicle length, the velocity of a vehicle can be approximated and the accuracy of the length estimate can be derived from the vehicle category parameter distribution. Table 2 shows representative numbers for the velocity error at typical sensor and car relative speeds (aircraft speed was 55 m/s and the car speed ranged between minimum and maximum freeway speed). As expected, the estimation error is smaller if the vehicle and the LiDAR are moving in the same direction (the measured length is longer at smaller relative speed). Another interpretation is that the relative impact of the fixed size of the car length range is smaller if it is compared to longer measured values, see Eq. 4. Although the velocity accuracy estimates are poor, the average velocity of a group of vehicles can be estimated significantly better as vehicles usually move at comparable speed plus the averaging process has an error cancellation character.

| Measured Length [m] | Velocity Accuracy [m/s] |
|---|---|
| 3 | 9.6 |
| 7 | 3.0 |
| 10 | 2.0 |
| 15 | 1.3 |

**Table 2.** The velocity error estimates based on measured vehicle length.

## 6. DENSITY AND FLOW PARAMETERS

Based on the computed vehicle locations and class categories, as well as estimated velocities, various flow parameters can be derived. Flow is typically computed as a product of average vehicle density and average vehicle velocity. Density is usually derived after calculating the average spacing of vehicles along a given lane/road by Equation 5. Spacing is the distance between the vehicles moving in the same direction, as measured between corresponding points (front to front) of consecutive vehicles.

$$Average \quad Space = \frac{\sum Space \quad Between \quad Vehicles}{Number \quad of \quad Vehicles} \qquad (5)$$

To illustrate the traffic flow computation process, data from a high-density (2-4 points/m$^2$) LiDAR survey, acquired on February 19, 2004, over the downtown Toronto area with the Optech ALTM 30/70 system, were used. Fig. 11 shows a highway segment with vehicles extracted from the LiDAR data and overlaid on the orthoimage. Note that the LiDAR point cloud of the vehicles falls before the vehicles in the left side and after the vehicles on the right, respectively. A red mark shows the likely location of the LiDAR beam when the image was taken. For referencing, static objects were also overlaid – one point at the centerline and points at the guard rail.

**Figure 11.** Vehciles extracted from LiDAR data overlaid on the orthoimage.

As the road is in a relatively flat area, only the horizontal components were used to compute the various flow parameters. The errors in spacing computation due to the non-instantaneous LiDAR data are ignored – this is acceptable if the relative speed of the vehicles is not changing rapidly. Table 3 lists the results, grouped by lane and road sides. Note that while vehicle velocity estimates are accurate to about 20%, the final flow has about 12% accuracy.

| Lane No. | Space [m] | Vel. [mile/h] | Density [Veh/mile] | Flow [Veh/h] |
|---|---|---|---|---|
| L1 | 24.5 | 50 | 66 | 3234 |
| L2 | 29.6 | 47 | 54 | 2646 |
| L3 | 24.9 | 48 | 57 | 2793 |
| **Total** | **8.7** | **49** | **177** | **8673** |
| | | **± 10** | **± 0.2** | **± 1100** |

**Table 3**: Traffic flow data

## 7. CONCLUSION

Our experiences with using LiDAR for obtaining traffic flow data have shown encouraging results. The developed concept and its prototype implementation proved that high-point density LiDAR can effectively support traffic monitoring and management by delivering a variety of traffic flow data. The proposed system represents an add-on capability to existing infrastructure airborne LiDAR mapping. Basically, this technique extracts the vehicles during the process of the road surface extraction and modeling, and uses them as a source for obtaining traffic flow. The recent introduction of the reflectance information is expected to further improve the road extraction process, while the vehicle classification seems to be unaffected by the availability of intensity data.

## ACKNOWLEDGEMENTS

This research was partially supported by the NCRST-F program and by Ohio Department of Transportation. The authors would like to thank Woolpert LLC and Optech International for providing the LiDAR datasets.

## REFERENCES

1. Grejner-Brzezinska D., Toth C and Paska E., (2003): Airborne Remote Sensing: Redefining a Paradigm of Traffic Flow Monitoring, ION GPS 2003, Portland, September 24-27, 2003, CD-ROM.
2. Grejner-Brzezinska D., Toth C and Paska E., (2004): Airborne Remote Sensing Supporting Traffic Flow Estimates, Proc. of 3rd International Symposium on Mobile Mapping Technology, Kunming, China, March 29-31, 2004, CD-ROM.
3. Hu, X., and Tao, V., (2004): Extraction of Streets in Dense Urban Area from Segmented LiDAR data, The 4th International Symposium of Mobile Mapping Technology, Kunming, China, March 29-31, 2004, CD-ROM.
4. Ramprakash, V.L., (2003): Detection and estimation of Vehicular Movement on Highways using a LiDAR sensor, MS.C. Thesis, The Ohio State University.
5. Thomas, T. R., (1999): *Rough Surfaces*, Imperial College Press, pp: 100-110.
6. Toth, C., Barsi A. and Lovas T., (2003a): Vehicle Recognition From LiDAR Data, *International Archives of Photogrammetry and Remote Sensing*, Vol. XXXIV, part 3/W13, pp. 163-166.
7. Toth C., Grejner-Brzezinska D. and Lovas T. (2003b): Traffic Flow Estimates from LiDAR Data, Proc. ASPRS Annual Conference, May 5-9, pp. 203-212, CD ROM.
8. Toth C., Grejner-Brzezinska D. and Merry C., (2003c): Supporting Traffic Flow Management with High-Definition Imagery, Proc. Of Joint ISPRS Workshop on High Resolution Mapping from Space 2003, Hannover, Germany, Oct 6-8, 2003, CD ROM.
9. Toth, C. and Grejner-Brzezinska, D., (2004): Vehicle Classification from LiDAR Data to Support Traffic Flow Estimates, Proc. of 3rd International Symposium on Mobile Mapping Technology, Kunming, China, March 29-31, 2004, CD-ROM.
10. Wehr, A. – Lohr U. (1999): Airborne Laser Scanning – and Introduction and Overview, *ISPRS Journal of Photogrammetry and Remote Sensing*, 54, pp. 68-82.